JOURNAL OF GEOPHYSICAL RESEARCH, VOL. 104, NO. D20, PAGES 24,257–24,263, OCTOBER 27, 1999

Greenhouse gases and climatic states of minimum entropy production

Toni Pujol
Departament de Física, Universitat de Girona, Girona, Spain

Josep Enric Llebot
Física Estadística, Departament de Física, Facultat de Ciències, Universitat Autònoma de Barcelona, Bellaterra, Spain

Joaquim Fort
Departament de Física, Universitat de Girona, Girona, Spain

Abstract. The hypothesis of minimum entropy production is applied to a simple one-dimensional energy balance model and is analyzed for different values of the radiative forcing due to greenhouse gases. The extremum principle is used to determine the planetary "conductivity" and to avoid the "diffusive" approximation, which is commonly assumed in this type of model. For present conditions the result at minimum radiative entropy production is similar to that obtained by applying the classical model. Other climatic scenarios show visible differences, with better behavior for the extremal case.

1. Introduction

Energy balance models (EBMs) provide a global description of the climate system. Among them, thermodynamic one-dimensional (1-D) horizontal models have been extensively analyzed because of their appealing features, namely (1) the adoption of simple and understandable equations; (2) the definition of a few, but important, independent variables; and (3) the possibility of studying other parameters not directly related to the main climatic variables. However, these models are intrinsically limited, because of (1) the simplified equations adopted for the radiative field, (2) the low resolution applied, (3) the description of meridional heat fluxes by means of diffusive equations, and (4) the limited number of free variables.

The present paper is focused on the role of entropy production in the climate, which can be easily analyzed by using a standard 1-D thermodynamic EBM. Few papers in the climate system deal with this variable, in spite of the fact that it is of utmost thermodynamical importance [*Prigogine*, 1947]. Thus, if steady states reached by the climate satisfied an extremal condition for the entropy production, the main variables at any scenario would be simply obtained [see, e.g., *Paltridge*, 1975; *Mobbs*, 1982; *Wyant et al.*, 1988; *O'Brien*, 1997].

On the other hand, the climate entropy production is formed by two different contributions, due to material and radiative fields. In the case of radiative emission by a system with a nonuniform temperature distribution, material and radiative entropy production rates are completely analogous [*Fort and Llebot*, 1998]. In contrast, the radiative part of the climate entropy neither follows a Gibbs equation nor presents a bilinear form, simply because the radiation entropy is not only associated with the terrestrial temperature [*Li et al.*, 1994]. Therefore Prigogine's minimum principle of entropy production at steady states cannot be applied to the climate system [*Prigogine*, 1947].

The majority of studies involving entropy production as a relevant parameter in defining the climatic states are based on the hypothesis of maximum material entropy production, postulated by *Paltridge* [1975]. This principle has been applied to a 1-D box EBM, leading to reasonable results for current conditions [*O'Brien and Stephens*, 1995]. Moreover, the same model also leads to plausible solutions at the state of maximum total entropy production (i.e., material plus radiative parts), as well as at the state of minimum radiative entropy production [*Pujol and Llebot*, 1999a]. However, it is important to stress that a rigorous derivation of an extremal behavior at steady states has not so far been presented, except for a variety of specific cases [*Essex*, 1984].

Here we analyze a standard 1-D diffusive EBM, presented in section 2, which has been extensively used in several climatic studies without any mention of the climate entropy [e.g., *North*, 1975a, b; *Hyde et al.*, 1990; *Lee and North*, 1995]. We apply the principle of minimum radiative entropy production for different values of the radiative forcing of greenhouse gases, on the basis of Planck's results as discussed in section 3 [*Planck*, 1913]. The comparison between values at a minimum rate of radiative entropy production and those obtained by the classical model is carried out in section 4, where better behavior for the extremal case is observed.

Paper number 1999JD900458.
0148-0227/99/1999JD900458$09.00

2. Diffusive EBM With Greenhouse Gas Effect

The model used is based on North's diffusive EBM [*North*, 1975a, b]. Although more elaborated versions can be found, even in two dimensions, the global picture of current conditions in this simple 1-D spectral model becomes enough for our purposes. At stationary conditions the imbalance between absorbed solar radiation and outgoing terrestrial radiation equals the meridional convergence of heat fluxes.

2.1. Radiative Energy Fluxes

The longwave energy flux to space $H^+(T,c)$ can be approximated by a first-order expansion in the surface air temperature T and the logarithm of the atmospheric carbon dioxide concentration c [*Hoffert et al.*, 1980]

$$H^+(T,c) = A + BT - C\ln(c/c_o) \ , \qquad (1)$$

where A and B are constants (A = 214.2 W m^{-2}, B = 1.575 W m^{-2} K^{-1} [*Nicolis and Nicolis*, 1980]). In fact, several values of A and B can be found in the literature [e.g., *Kuhn et al.*, 1989; *Graves et al.*, 1993; *Caldeira and Kasting*, 1992]. For comparative purposes we have chosen A and B similar to those used in some papers that analyze the role of the entropy in the climate system [*Nicolis and Nicolis*, 1980; *Li and Chýlek*, 1994; *Pujol and Llebot*, 1999a].

The last term in (1) is the greenhouse gases (GHG) radiative forcing. A value for the coefficient C can be obtained from $C = 2.5B/\ln 2 \approx 5.7$ W m^{-2} [*Hoffert et al.*, 1980], which tries to reflect the best "estimate" sensitivity expected for the climate. However, other values of C have been proposed. For example, a value of C = 6.3 W m^{-2} has been obtained by *Mitchell et al.* [1995] and used by the Intergovernmental Panel on Climate Change (*IPCC*) [1995], whereas a value of C = 5 W m^{-2} has been more recently adopted by *Hewitt and Mitchell* [1997]. Since the present paper is not especially focused on one particular scenario, several values of the radiative forcing due to greenhouse gases will be analyzed. Thus the specific value of C becomes a somehow minor point because the sensitivity of the climatic variables to changes in C will be obtained.

In (1), T is expressed in degrees Celsius and c_o represents the greenhouse gas concentration at current conditions. On the other hand, the absorbed shortwave energy flux $H^-(x,\alpha)$, follows

$$H^-(x,\alpha) = F\,S(1-\alpha) \ , \qquad (2)$$

where x is the sine of the latitude, α is the albedo, F is the solar "constant" divided by 4 (340 W m^{-2}), and S is the insolation function, which decreases toward the pole.

2.2. Material Energy Fluxes

The meridional energy flux $\boldsymbol{Q}$ is obtained by using a diffusive approach, which yields

$$\boldsymbol{Q}\ (T) = -\lambda_Q \nabla T \ , \qquad (3)$$

with λ_Q a given constant planetary "conductivity," chosen as λ_Q = 0.591 W m^{-2} K^{-1} for current conditions [*Nicolis and Nicolis*, 1980]. The gradient operator in (3) is dimensionless, following

$$\nabla = \boldsymbol{a}_x \left(1-x^2\right)^{1/2} \frac{\partial}{\partial x} \ , \qquad (4a)$$

whereas

$$\nabla\cdot = \boldsymbol{a}_x \frac{\partial \left(1-x^2\right)^{1/2}}{\partial x} \ , \qquad (4b)$$

holds for the divergence, $\boldsymbol{a}_x$ being a unit vector toward the pole.

2.3. Latitudinal Dependence of Variables and Parameters

The latitudinal variation of the parameters is prescribed, following *North* [1975b], as

$$T(x) = T_0 + T_2 P_2(x) \ , \qquad (5a)$$

$$S(x) = 1 + S_2 P_2(x) \ , \qquad (5b)$$

$$\alpha(x) = \alpha_0 + \alpha_2 P_2(x) \ , \qquad (5c)$$

where $P_2(x)$ is the second-order Legendre polynomial. First-order terms drop out by taking symmetric hemispheres into account. Thus T_0 is the planetary, globally averaged temperature in °C. T_2 is two thirds the difference between the temperature of the poles and that of the equator, and $S_2 = -0.477$.

Equation (5c) is used for latitudes below the ice sheet edge (α_0 = 0.303, α_2 = 0.0779), whereas above this boundary a constant albedo (equal to the ice value ≈ 0.62) is assumed. Moreover, the ice sheet edge x_s is defined as the sine of the latitude where the surface temperature becomes −10°C (i.e., $T(x_s)$ = −10°C).

2.4. Steady State Equations

The temperature and the ice sheet edge are the only free variables in the model. At stationary conditions, T_0, T_2, and x_s are obtained by solving the following:

$$A + B\,T_0 - C\ln(c/c_o) = F\,I_0(x_s) \ , \qquad (6)$$

$$(B + 6\lambda_Q)T_2 = F\,I_2(x_s) \ , \qquad (7)$$

$$T_0 + T_2 P_2(x_s) = -10°\mathrm{C} \ , \qquad (8)$$

where $I_m(x_s)$ is given by

$$I_m(x_s) = (2m+1)\int_0^1 dx\, S(x)\left[1-\alpha(x,x_s)\right]P_m(x) \ , \quad m = 0, 2 \ . \qquad (9)$$

Equation (6) has been obtained by averaging over the whole globe the energy balance equation, namely,

$$\nabla\cdot\boldsymbol{Q} = H^- - H^+ \ . \qquad (10)$$

Moreover, (7) is the globally averaged result of multiplying (10) by $P_2(x)$, taking the orthogonal properties of the Legendre polynomials into account. Finally, (8) represents the explicit condition for evaluating the ice sheet edge x_s.

Results for current conditions ($c = c_o$) imply a globally averaged temperature T_0 = 14.9°C, a pole-equator temperature difference of −42.3°C and an ice sheet edge x_s = 0.96 (≈ 73.7° of latitude).

Any variation in greenhouse gases would lead to a change in temperature as well as in ice sheet edge. Nevertheless, there is no reason to assume a constant value for the planetary conductivity λ_Q because the climate dynamics at other scenarios can differ from the current one. Thus Figures 1a and 1b show the values for λ_Q and the changes in globally averaged temperature T_0 (relative to the present value) as functions of the ice sheet edge and the radiative forcing due to greenhouse gases (GHG radiative forcing). Values shown in Figure 1 have been derived as follows. Equation (6) relates T_0 to x_s and c (this has been used to obtain Figure 1b). Equation (8) relates T_2 to T_0 and x_s. Thus these two equations can be used to relate T_2 to x_s and c. Combining this dependence with (7) (which relates λ_Q to x_s and T_2) allows us to relate λ_Q to x_s and c (Figure 1a), because the solar insolation F has been kept fixed.

By applying the classical climate model described above, the changes in temperature due to variations in greenhouse gas forcing would follow the isoline of $\lambda_Q = 0.591$ W m^{-2} K^{-1}. Thus, for a radiative forcing of only ≈ 0.75 W m^{-2}, an ice-free Earth would be obtained with an increase in globally averaged temperature ≈ 1.6°C. Hence a given variation in λ_Q would improve the climatic states obtained by using a simple 1-D diffusive EBM at future scenarios. However, if the heat fluxes are kept as free variables (i.e., if λ_Q is no longer fixed), an additional constraint must be included in the system. We tackle this problem by making use of the principle of minimum radiative entropy production, which is presented in the next section, as an additional constraint.

3. Minimum Radiative Entropy Production

Essex [1984], based on one of Planck's results [*Planck*, 1913], has analytically proved the application of the principle of minimum radiative entropy production in several systems in radiative equilibrium, among them, a continuos atmosphere including both material and radiation fields. Therefore this principle is of interest within the framework of stellar theory, and it may also be a useful tool in the study of the climate, although it is not in radiative equilibrium at a given latitudinal point.

However, the steady state of a global picture of the climate is, in fact, in radiative equilibrium. In consequence, one could expect that the principle of minimum radiative entropy production could successfully be applied to the climate when a simple and schematic climate model is used.

Indeed, we show how a simple picture of the climate system (based on a 1-D diffusive model where the convective fluxes are not taken into account) is able to follow such an extremal behavior. First, it is convenient to define the components of climatic entropy.

3.1. Entropy Production

At stationary conditions the total entropy production $\mathcal{P}_t$ (matter plus radiation) becomes

$$\mathcal{P}_t = \nabla \cdot \boldsymbol{J} - \frac{\nabla \cdot \boldsymbol{H}}{\mathcal{T}} + \boldsymbol{Q} \cdot \nabla \frac{1}{\mathcal{T}}, \tag{11}$$

where $\boldsymbol{J}$ and $\boldsymbol{H}$ are the entropy and energy fluxes of radiation, respectively [*Pujol and Llebot*, 1999b], and $\mathcal{T}$ is the temperature in kelvins ($\mathcal{T} = T + 273$). The last term on the right-hand side of (11) is the expression for the entropy production due to material fluxes, namely,

$$\mathcal{P}_m = \boldsymbol{Q} \cdot \nabla \frac{1}{\mathcal{T}}, \tag{12}$$

which has been extensively analyzed in several thermodynamic systems [*Jou et al.*, 1996]. Also in the climate system,

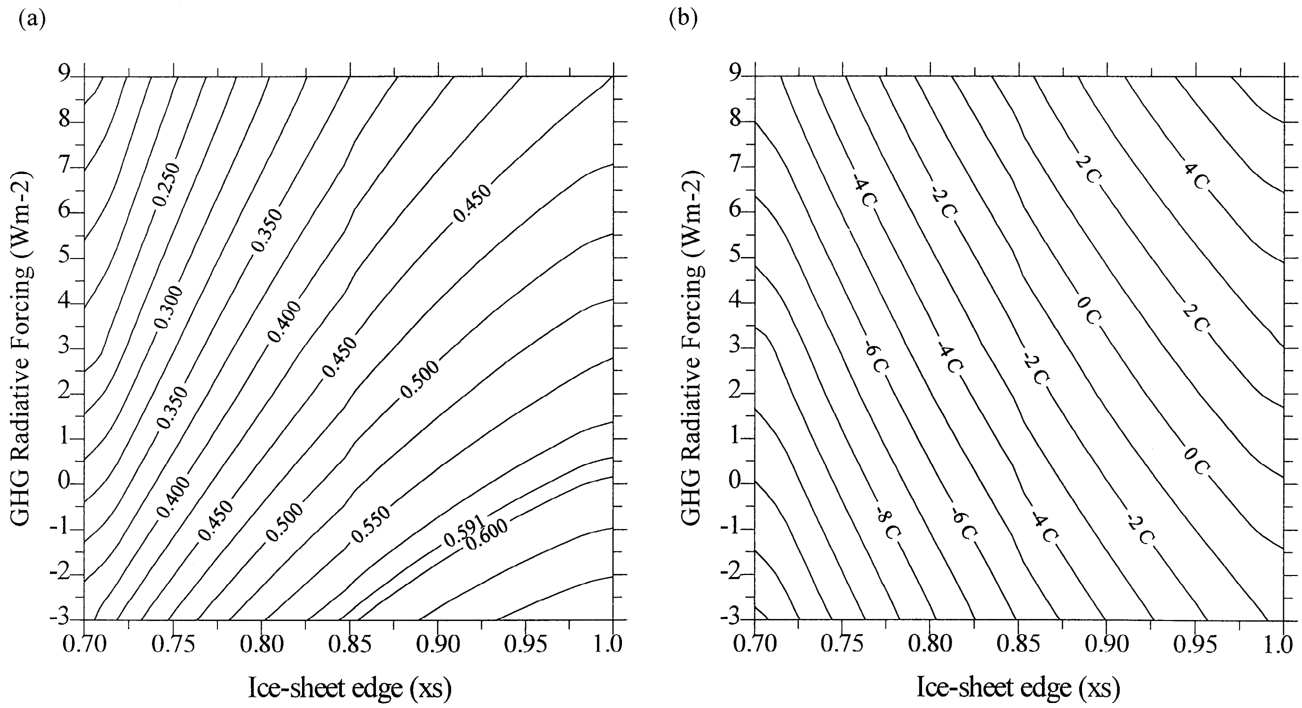

Figure 1. (a) Planetary "conductivity" λ_Q (W m^{-2} K^{-1}) and (b) globally averaged changes in temperature (°C) dependence on the ice sheet edge (sine of the ice sheet latitude) and the greenhouse gas (GHG) radiative forcing (last term in equation (1)). Values for a usual procedure in the energy balance model analyzed would follow the isoline of $\lambda_Q = 0.591$ W m^{-2} K^{-1}. Climatic states at minimum radiative entropy production present variations in λ_Q.

$\mathcal{P}_m$ has a bilinear form, provided that a diffusive approach for the total material heat flux $\boldsymbol{Q}$ is assumed.

At stationary conditions the meridional integration of (12) yields

$$\int_0^1 \frac{\nabla\cdot\boldsymbol{Q}}{\mathcal{T}}dx = -\int_0^1 \boldsymbol{Q}\cdot\nabla\frac{1}{\mathcal{T}}dx, \qquad (13)$$

where x is the sine of the latitude, since $\boldsymbol{Q}$ vanishes at poles and equator. Thus the meridional integration of $\mathcal{P}_t$ equals the entropy fluxes across the boundary of the system, because the last two terms on the right-hand side of the meridional integration of (11) cancel out, since they are the same as those appearing in the energy balance equation (10) after it is integrated over the latitude and divided by $\mathcal{T}$. Moreover, we have applied that $\nabla\cdot\boldsymbol{H}$ becomes the difference between H^+ and H^- within the 1-D model used. These fluxes are given by (1) and (2), respectively. We stress that the radiation flux of entropy $\boldsymbol{J}$ is not linearly related to the radiation flux of energy $\boldsymbol{H}$ [see also *Pujol and Llebot*, 1999b].

Finally, from (11) and (12), the radiative entropy production is [*Li and Chýlek*, 1994]

$$\mathcal{P}_r = \nabla\cdot\boldsymbol{J} - \frac{\nabla\cdot\boldsymbol{H}}{\mathcal{T}}. \qquad (14)$$

3.2. Extremal States

At the steady state the terms involving the meridional heat flux $\boldsymbol{Q}$ in $\mathcal{P}_t$ and $\mathcal{P}_m$ can be obtained from (10), in which the latitudinal distribution of temperatures is not prescribed. Thus $\mathcal{P}_t$ and $\mathcal{P}_m$ do not involve any planetary conductivity. Hence, for a given ice sheet edge, the temperature distribution that maximizes both $\mathcal{P}_t$ and $\mathcal{P}_m$ is obtained. *Pujol and Llebot* [1999b] found that the climatic state maximizing $\mathcal{P}_t$ ($\mathcal{P}_{tm}$, say) corresponds to an isothermal distribution, whereas the maximum in $\mathcal{P}_m$ ($\mathcal{P}_{mm}$, say) presents a higher latitudinal variation than current values. Moreover, comparison of the values obtained for both $\mathcal{P}_{tm}$ and $\mathcal{P}_{mm}$ to those for $\mathcal{P}_t$ and $\mathcal{P}_m$, corresponding to the present state, indicate that the current climate does not follow maximum behavior, neither in total nor in matter entropy production within *North*'s [1975a, b] 1-D model. However, the climate seems to tend to a given state where the extreme of the difference between $\mathcal{P}_{tm}$ and $\mathcal{P}_{mm}$ ($\mathcal{P}_{rm}$, say) equals the value for the radiative entropy production $\mathcal{P}_r$. We shall here refer to $\mathcal{P}_{rm}$ as the minimum radiative entropy production, following *Pujol and Llebot* [1999a], who found that the state of minimum radiative entropy production in Paltridge's 1-D box model is nearly equivalent to the states that satisfy both $\mathcal{P}_{tm}$ or $\mathcal{P}_{mm}$ conditions.

4. Results

Differences between $\mathcal{P}_{rm}$ and $\mathcal{P}_r$ in function of the ice sheet edge for different values of GHG radiative forcing are shown in Figure 2. By making use of the hypothesis of minimum radiative entropy production, the climatic state (i.e., the ice sheet edge and temperature) has been determined such that its value of $\mathcal{P}_r$ equals to $\mathcal{P}_{rm}$ or, if this is not possible, that the difference between both becomes minimum. Moreover, for a given value of the GHG radiative forcing, two possible states where $\mathcal{P}_r = \mathcal{P}_{rm}$ have been found. In this case and according to the hypothesis above, the state with the minimum value of radiative entropy production has been selected. For current conditions ($c = c_o$) the minimum climatic state in $\mathcal{P}_r$ - $\mathcal{P}_{rm}$ leads to 14.8°C for the globally averaged temperature T_0, −28.5°C for T_2 (= −42.75°C for the pole-equator temperature difference), 0.955 for the ice sheet edge (≈ 72.7° latitude), and 0.588 W m^{-2} K^{-1} for the planetary conductivity. Such values are in close agreement with those corresponding to the current state obtained from the standard diffusive model (see the second paragraph below (10)). However, some differences arise in the analysis of future scenarios, where the GHG radiative forcing is expected to present a considerable increase. Table 1 summarizes the results obtained through applying the hypothesis of minimum radiative entropy production for several values of the internal forcing. For example, the results for current conditions (given above) correspond to the fourth row in Table 1. For comparison purposes, Table 2 presents the values obtained by using the standard 1-D model presented in section 2 (i.e., by assuming a constant planetary conductivity λ_Q = 0.591 W m^{-2} K^{-1}). For example, the results for current conditions (given below (10)) correspond to the fourth row in Table 2.

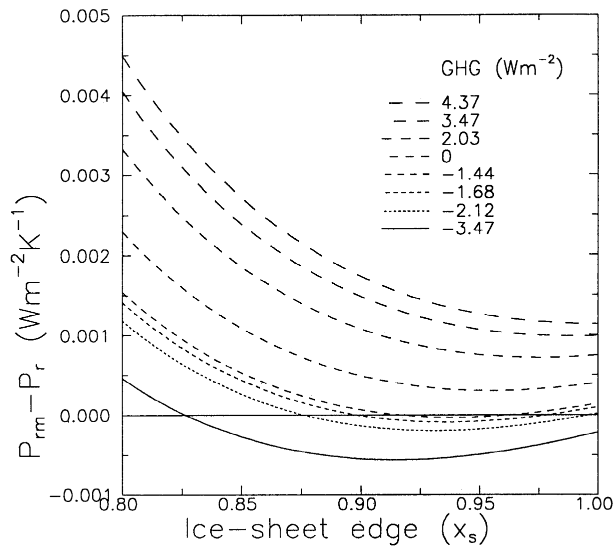

Figure 2. Differences between minimum radiative entropy production $\mathcal{P}_{rm}$ and radiative entropy production $\mathcal{P}_r$ as a function of the ice sheet edge and for different values of radiative forcing due to greenhouse gases.

The GHG radiative forcing corresponds to a doubling of CO_2 concentration for a value of C = 6.3 W m^{-2} (GHG radiative forcing ≈ 4.37 W m^{-2} [*Mitchell et al.*, 1995]) or C = 5 W m^{-2} (GHG radiative forcing ≈ 3.47 W m^{-2} [*Hewitt and Mitchell*, 1997]). For the latter value of C, results at 1.5, 0.75, and 0.5 times the present concentration of greenhouse gases c_o are also shown in Tables 1 and 2. Moreover, the GHG radiative forcing corresponding to the Last Glacial Maximum (LGM) has also been included. In this case, the variation of the last term in (1) has been assumed to be ≈ C ln (200/280) [see *Hewitt and Mitchell*, 1997], and the results are shown for C = 5 and 6.3 W m^{-2}.

4.1. Temperature and Ice Sheet Changes

The usual procedure in the standard 1-D model yields a high warming until reaching the ice-free Earth; afterward, a

Table 1. Results for Several Greenhouse Gas Radiative Forcings at the State of Minimum Rate of Radiative Entropy Production

C, W m-2	c/c_o	$\Delta[C \ln(c/c_o)]$, W m-2	T_0, °C	ΔT_0, °C	T_2, °C	Ice Sheet Edge, deg	λ_Q, W m-2 K-1	$F\Delta I_0(x_s)$, W m-2	χ_{GHG}, K m2 W-1	χ_{xs}, K m2 W-1
6.3	2	4.4	18.8	4.0	-29.0	86.4	0.52	2.0	0.9	2.1
5	2	3.5	18.0	3.2	-28.6	81.9	0.54	1.6	0.9	2.0
5	1.5	2.0	16.7	1.9	-28.7	77.4	0.56	1.0	0.9	2.0
-	1	-	14.8	-	-28.5	72.7	0.59	-	-	-
5	0.75	-1.4	12.6	-2.2	-29.6	66.5	0.60	-2.0	1.5	1.1
5	200/280*	-1.7	11.8	-3.0	-30.6	64.0	0.60	-3.1	1.8	1.0
6.3	200/280	-2.1	10.6	-4.2	-31.6	61.2	0.59	-4.4	2.0	0.9
5	0.5	-3.5	7.6	-7.2	-33.7	55.7	0.59	-7.7	2.1	0.9

Parameters are defined in the text. The greenhouse gas (GHG) radiative forcing is represented as $\Delta[C \ln(c/c_o)]$; ΔT_0 is the change in globally averaged temperature T_0 relative to the result of the model for the current state (14.8°C). Global climate sensitivity is $1/B = 1/(\chi_{GHG}^{-1} + \chi_{xs}^{-1})$ (± 0.04 K m2 W-1 with the accuracy of χ_{GHG} and χ_{xs} used).

* Value is assumed to be equivalent to the Last Glacial Maximum to present conditions [*Hewitt and Mitchell*, 1997].

lower rate of temperature increase is obtained. The minimum radiative forcing that leads to an ice-free Earth is only ≈ 0.75 W m-2, corresponding to a globally averaged warming ≈ 1.6°C.

More reasonable values appear in the case of minimum radiative entropy production, where an ice-free Earth is not reached even for the maximum radiative forcing adopted (see Table 1). From this perspective it is merely fortuitous that the value of T_0 at the $2CO_2$ state is close to that obtained by using the standard EBM with fixed planetary conductivity. The changes in globally averaged temperature become important, being in the range of 3.2°-4.0°C, depending on the GHG radiative forcing chosen for the scenario of doubling the CO_2 concentration. These figures agree, for example, with *Stocker and Schmittner* [1997], who found a value ≈ 3.7°C using an EBM coupled to an oceanic global climate model (GCM), and with *Reader and Boer* [1998], who found a value ≈ 3.4°C using the GCMII of the Canadian Centre for Climate Modelling and Analysis (CCCma).

For a negative GHG radiative forcing the climatic states obtained through the minimum principle of entropy production become similar to those found by using the standard model (rows 5–8 in Tables 1 and 2, respectively). As a special case, the cooling corresponding to the LGM lies between −3.0°C and −4.2°C, depending on the value assumed for C. Although this variation in temperature is similar (in absolute value) to that found for the $2CO_2$ state, the GHG radiative forcing in that case was almost two times higher. Changes in temperature at the LGM from proxy data and from GCMs lie in the interval between −3.0°C and −5.0°C [*Broccoli and Manabe*, 1987; *Hoffert and Covey*, 1992; *Hewitt and Mitchell*, 1997].

4.2. Planetary Conductivity and Meridional Temperature Gradient

The standard 1-D model relies on a fixed value for the planetary conductivity, namely, λ_Q = 0.591 W m-2 K-1, whereas the model based on the constraint of minimum rate of radiative entropy production allows for different values of λ_Q. As is seen from Table 1, for negative GHG radiative forcings, the planetary conductivity is similar to that obtained for the present value and used in *North*'s [1975a, b] model. However, for positive values of the GHG radiative forcing, the planetary conductivity decreases substantially. Therefore meridional

Table 2. Results for Several Greenhouse Gas Radiative Forcings by Following the Usual Procedure, λ_Q = 0.591 W m-2 K-1)

C, W m-2	c/c_o	$\Delta[C \ln(c/c_o)]$, W m-2	T_0, °C	ΔT_0, °C	T_2, °C	Ice Sheet Edge, deg	$F\Delta I_0(x_s)$, W m-2	χ_{GHG}, K m2 W-1	χ_{xs}, K m2 W-1
6.3	2	4.4	18.8	3.9	-26.6*	90.0†	1.8‡	0.9	2.1 (0.9‡)
5	2	3.5	18.2	3.2	-26.6*	90.0†	1.8‡	1.0	1.8 (0.9‡)
5	1.5	2.0	17.3	2.4	-26.6*	90.0†	1.8‡	1.2	1.3 (0.9‡)
-	1	-	14.9	-	-28.2	73.7	-	-	-
5	0.75	-1.4	11.9	-3.0	-30.8	64.0	-3.3	2.1	0.9
5	200/280	-1.7	11.4	-3.5	-31.1	62.9	-3.8	2.1	0.9
6.3	200/280	-2.1	10.5	-4.4	-31.8	60.9	-4.8	2.1	0.9
5	0.5	-3.5	7.7	-7.2	-33.5	55.9	-7.8	2.1	0.9

Parameters are defined in the text. The GHG radiative forcing is represented as $\Delta[C \ln(c/c_o)]$; ΔT_0 is the change in globally averaged temperature T_0 relative to the result of the model for the current state (14.9°C). Global climate sensitivity is $1/B = 1/(\chi_{GHG}^{-1} + \chi_{xs}^{-1})$ (± 0.04 K m2 W-1 with the accuracy of χ_{GHG} and χ_{xs} used).

* Value is same as that obtained for an ice-free Earth.

† An ice-free Earth is obtained for a GHG radiative forcing = 0.75 W m-2 or higher.

‡ These values correspond to the variation between the current state and that obtained with a GHG radiative forcing = 0.75 W m-2. Values in parentheses are those considered before an ice-free Earth is reached.

heat transport is reduced, which agrees with usual predictions carried out by GCMs [*IPCC*, 1995].

From the values of T_2 in Table 1, we see that the pole-equator temperature gradient presents slight changes for an enhancement in greenhouse gases ($c > c_o$) when the hypothesis of minimum radiative entropy production is adopted. However, a reduction in greenhouse gases with respect to the present value ($c < c_o$) implies a clear trend to increase the pole-equator gradient of temperatures. On the other hand, the standard 1-D model, with a constant value for λ_Q, always predicts an increase in T_2 (i.e., decrease in pole-equator gradient of temperatures) for an increase in T_0.

4.3. Ice Sheet Radiative Forcing

Any variation in the ice sheet edge obtained for a given climatic scenario produces a particular change in the globally averaged shortwave radiative forcing (6). Thus the ice sheet radiative forcing, namely, $F\,\Delta I_0(x_s)$, is shown in both Tables 1 and 2. This depends only on the variation of the ice sheet edge if F remains constant. By doubling the CO_2, the ice sheet radiative forcing becomes between 1.6 and 2.0 W m^{-2}, depending on the value of C that has been assumed. On the other hand, changes in the ice sheet edge for the LGM lead to an ice sheet radiative forcing within the range −3.1 W m^{-2} and −4.4 W m^{-2}, values which are higher than those obtained by using GCMs (e.g., ≈ −2.9 W m^{-2} [*Hewitt and Mitchell*, 1997]). In this case, however, the sum of the ice sheet plus the GHG radiative forcings in Table 1 is in agreement with the range obtained from proxy data and simulated by GCMs (between −4.7 and −6.6 W m^{-2}).

4.4. Climate Sensitivity

The climate sensitivity χ, defined as

$$\chi = \frac{\Delta T_0}{\Delta H}, \qquad (15)$$

can be analyzed by noting that (6) links the changes in T_0 to variations in the energy fluxes, which we denote by ΔH,

$$B\Delta T_0 = \Delta[C\ln(c/c_o)] + F\Delta I_0(x_s) \equiv \Delta H\,. \qquad (16)$$

In Tables 1 and 2 the changes due to both energy fluxes have been analyzed separately. Thus the value of χ_{GHG} refers to the changes in the outgoing longwave radiation due to greenhouse gases (here ΔH corresponds to $\Delta[C\ \ln(c/c_o)]$), whereas χ_{xs} is related to the changes in ice sheet edge (so that ΔH corresponds to $F\ \Delta I_0(x_s)$). Therefore $B = \chi_{\mathrm{GHG}}^{-1} + \chi_{\mathrm{xs}}^{-1}$ from (16).

Both changes in globally averaged temperature ΔT_0 and longwave energy fluxes ΔH appearing in (15) are taken in reference to current conditions (i.e., relative to the case $c/c_o = 1$ in Tables 1 and 2).

For levels of greenhouse gases that are not great enough to produce an ice-free Earth, the standard 1-D model (Table 2) presents a climate sensitivity $\chi_{\mathrm{GHG}} \approx 2.1$ K m^2 W^{-1}, which has been obtained from the values of ΔT_0 and $\Delta[C\ \ln(c/c_o)]$ shown in Table 2. This value for χ_{GHG} is higher than those found by GCMs (≈ 0.4 – 1.1 K m^2 W^{-1} [*Cess et al.*, 1989]). Beyond a GHG radiative forcing of 0.75 W m^{-2}, the climate sensitivity χ_{GHG} becomes lower because an ice-free Earth is reached. In this case, the value of χ_{GHG} contains two types of contributions,

$$\chi_{\mathrm{GHG}} = \frac{\Delta T_0}{\Delta[C\ln(c/c_o)]} = \frac{\Delta^{\mathrm{iv}}T_0 + \Delta^{\mathrm{if}}T_0}{\Delta^{\mathrm{iv}}[C\ln(c/c_o)] + \Delta^{\mathrm{if}}[C\ln(c/c_o)]}, \qquad (17)$$

where the contributions denoted by the superscript iv (ice variable) refer to the variations from present conditions until reaching an ice-free (if) Earth. Until this point, $\chi_{\mathrm{GHG}}{}^{\mathrm{iv}}$ reads

$$\chi_{\mathrm{GHG}}{}^{\mathrm{iv}} = \frac{\Delta^{\mathrm{iv}}T_0}{\Delta^{\mathrm{iv}}[C\ln(c/c_o)]} \approx 2.1 \text{ K m}^2\text{ W}^{-1}\,. \qquad (18)$$

The second type of contribution in (17), denoted by the superscript if (ice free), corresponds to the variation from the initial point where the ice-free Earth has been reached, until the final state specified. In this stage, $x_s = 1$ is fixed, thus we have from (9) that $\Delta I_0(x_s) = 0$ and (16) become $B\ \Delta^{\mathrm{if}}T_0 = \Delta^{\mathrm{if}}\ [C\ \ln(c/c_o)]$. Thus in the ice-free stage, $\chi_{\mathrm{GHG}}{}^{\mathrm{if}}$ reduces to

$$\chi_{\mathrm{GHG}}{}^{\mathrm{if}} = \frac{\Delta^{\mathrm{if}}T_0}{\Delta^{\mathrm{if}}[C\ln(c/c_o)]} = \frac{1}{B} \approx 0.6 \text{ K m}^2\text{ W}^{-1}\,, \qquad (19)$$

where we have made use of the value for B given below (1). The fact that $\chi_{\mathrm{GHG}}{}^{\mathrm{if}} < \chi_{\mathrm{GHG}}{}^{\mathrm{iv}}$ leads to a lower climate sensitivity on the greenhouse gas concentration in the top three rows in Table 2 (where the values of χ_{GHG} have been obtained from (17)). Similarly, the climate sensitivity due to changes in the ice sheet radiative forcing is

$$\chi_{\mathrm{xs}} = \frac{\Delta T_0}{F\Delta I_0(x_s)} = \frac{\Delta^{\mathrm{iv}}T_0 + \Delta^{\mathrm{if}}T_0}{F\Delta^{\mathrm{iv}}I_0(x_s)} = \frac{\Delta^{\mathrm{iv}}T_0}{F\Delta^{\mathrm{iv}}I_0(x_s)} + \frac{\Delta^{\mathrm{if}}T_0}{F\Delta^{\mathrm{iv}}I_0(x_s)}\,. \qquad (20)$$

In the last column in Table 2 we give the values of χ_{xs} obtained from this equation and, in parentheses, the corresponding values when only the variation until an ice-free Earth is considered (i.e., the first term on the right-hand side of (20)). As may be seen from Table 2, this change is the same as that obtained in those simulations in which the changes in GHG concentration do not produce an ice-free Earth, as they should.

In comparison, the climate sensitivity χ_{GHG} found by applying the minimum radiative entropy production decreases when the GHG radiative forcing increases (Table 1). For example, at the state of doubling the CO_2 concentration, $\chi_{\mathrm{GHG}} \approx$ 0.9 K m^2 W^{-1}, which is similar to that value obtained by *Hewitt and Mitchell* [1997] by using a GCM, whereas the climate sensitivity at LGM becomes ≈ 1.9 K m^2 W^{-1}, which agrees with that obtained from proxy data [*Hoffert and Covey*, 1992]. Moreover, both standard and extremum procedures lead to similar values for the climate sensitivity at LGM conditions. Finally, the simplicity of the model must be stressed, which implies that the numerical results found should be regarded as useful for illustrative purposes but not of absolute validity.

5. Conclusions

Planck's principle of minimum radiative entropy production has been shown to hold strictly for a series of specific systems, although a completely general proof is still lacking [see, e.g., *Essex*, 1984]. This principle has been applied here to a simple 1-D EBM [*North*, 1975a, b], so that the diffusive approach can be removed. Thus, whereas a usual approach to the standard 1-D model fixes the value of the planetary conductivity, the hypothesis of minimum radiative entropy production provides this parameter as a function of the radiative forcing applied. For current conditions the climate at the minimum radiative entropy production is similar to that obtained by the standard application of the model. However, for a moderate positive radiative forcing of greenhouse gases, the climate predicted from the hypothesis of minimum radiative entropy production presents a lower coefficient for the planetary conductivity, producing a reduction in meridional heat transport and avoiding the ice-free Earth predicted by the standard model. Moreover, the climate sensitivity due to changes in greenhouse gases becomes similar to that obtained by GCMs, although it increases for a reduction in their concentration. On the other hand, the conductivity corresponding to meridional heat transport remains nearly unchanged for a reduction in greenhouse gas concentration.

Acknowledgments. This work has been partially supported by the Ministerio de Educación y Cultura of the Spanish Government under contracts CLI95-1867 and PB96-0451.

References

Broccoli, A.J., and S. Manabe, The influence of continental ice, atmospheric CO_2, and land albedo on the climate of the last glacial maximum, *Clim. Dyn.*, *1*, 87-99, 1987.

Caldeira, K., and F. Kasting, Susceptibility of the early Earth to irreversible glaciation caused by carbon dioxide clouds, *Nature*, *359*, 226-228, 1992.

Cess, R. D., et al., Interpretation of cloud-climate feedback as produced by 14 atmospheric general circulation models, *Science*, *241*, 513-516, 1989.

Essex, C., Minimum entropy production in steady state and radiative transfer, *Astrophys. J.*, *285*, 279-293, 1984.

Fort, J., and J.E. Llebot, Information-theoretical derivation of an extended termodynamical description of radiative systems, *J. Math. Phys.*, *39*, 345-354, 1998.

Graves, C.E., W.-H. Lee, and G.R. North, New parameterizations and sensitivities for simple climate models, *J. Geophys. Res.*, *98*, 5025-5036, 1993.

Hewitt, C.D., and J.F.B. Mitchell, Radiative forcing and response of a GCM to ice age boundary conditions: Cloud feedback and climate sensitivity, *Clim. Dyn.*, *13*, 821-834, 1997.

Hoffert, M.I., and C. Covey, Deriving global climate sensitivity from palaeoclimate reconstructions, *Nature*, *360*, 573-576, 1992.

Hoffert, M.I., A.J. Callegari, and C.-T. Hsieh, The role of deep sea heat storage in the secular response to climatic forcing, *J. Geophys. Res.*, *85*, 6667-6679, 1980.

Hyde, W.T., K.-Y. Kim, T. J. Crowley, and G. R. North, On the relation between polar continentality and climate: Studies with a nonlinear seasonal energy balance model, *J. Geophys. Res.*, *95*, 18,653-18,668, 1990.

Intergovernmental Panel on Climate Change, *Climate Change 1995: The Science of Climate Change*, edited by J.T. Houghton et al., Cambridge Univ. Press, New York, 1995.

Jou, D., Casas-Vázquez J., and G. Lebon, *Extended Irreversible Thermodynamics*, Springer-Verlag, Berlin, Germany, 1996.

Kuhn, W.R., J.C.G. Walker, and H.G. Marshall, The effect on Earth's surface temperature from variations in rotation rate, continent formation, solar luminosity, and carbon dioxide, *J. Geophys. Res.*, *94*, 11,129-11,136, 1989.

Lee, W.-H., and G. R. North, Small ice cap instability in the presence of fluctuations, *Clim. Dyn.*, *11*, 242-246, 1995.

Li, J., and P. Chýlek, Entropy in climate models, II; Horizontal structure of atmospheric entropy production, *J. Atmos. Sci.*, *51*, 1702-1708, 1994.

Li, J., P. Chýlek, and G. B. Lesins, Entropy in climate models, I; Vertical structure of atmospheric entropy production, *J. Atmos. Sci.*, *51*, 1691-1701, 1994.

Mitchell, J.F.B., T.C. Johns, J. M. Gregory, and S.F.B. Tett, Climate response to increasing levels of greenhouse gases and sulphates aerosols, *Nature*, *376*, 501-504, 1995.

Mobbs, S. D., Extremal principles for global climate models, *Q. J. R. Meteorol. Soc.*, *108*, 535-550, 1982.

Nicolis, G., and C. Nicolis, On the entropy balance of the Earth-atmosphere system, *Q. J. R. Meteorol. Soc.*, *106*, 691-706, 1980.

North, G. R., Analytical solution to a simple climate model with diffusive heat transfer, *J. Atmos. Sci.*, *32*, 1301-1307, 1975a.

North, G. R., Theory of energy-balance models, *J. Atmos. Sci.*, *32*, 2033-2043, 1975b.

O'Brien, D. M., A yardstick for global entropy-flux, *Q. J. R. Meteorol. Soc.*, *123*, 243-260, 1997.

O'Brien, D.M., and G.L. Stephens, Entropy and Climate, II; Simple models, *Q. J. R. Meteorol. Soc.*, *121*, 1773-1796, 1995.

Paltridge, G. W., The steady-state format of global climate, *Q. J. R. Meteorol. Soc.*, *104*, 927-945, 1975.

Planck, M., *The Theory of Heat Radiation*, 2nd ed., Dover, New York, 1913.

Prigogine, I., *Etude Thermodynamique des Phénomènes Irreversibles*, Desoer, Liège, Belgium, 1947.

Pujol, T., and J.E. Llebot, Extremal principle of entropy production in the climate system, *Q. J. R. Meteorol. Soc.*, *125*, 79-90, 1999a.

Pujol, T., and J.E. Llebot, Second differential of the entropy as a criteria for the stability in low-dimensional climate models, *Q. J. R. Meteorol. Soc.*, *125*, 91-106, 1999b.

Reader, M.C., and G. J. Boer, The modification of greenhouse gas warming by the direct effect of sulphate aerosols, *Clim. Dyn.*, *14*, 593-607, 1998.

Stocker, T.F., and A. Schmittner, Influence of CO_2 emission rates on the stability of the thermohaline circulation, *Nature*, *388*, 862-865, 1997.

Wyant, P. H., A. Mongroo, and S. Hameed, Determination of the heat-transport coefficient in Energy-Balance Climate Models by extremisation of entropy production, *J. Atmos. Sci.*, *45*, 189-193, 1988.

J. Fort, and T. Pujol, Departament de Física, Universitat de Girona, Campus Montilivi, 17071 Girona, Catalonia, Spain. (e-mail: caaps@fc.udg.es)

J. E. Llebot, Física Estadística, Departament de Física, Universitat Autònoma de Barcelona, 08193 Bellaterra, Catalonia, Spain.

(Received December 21, 1998; revised June 2, 1999;
accepted June 15, 1999.)